**Referee #2:**

**Summary:**

A newly developed ship-borne wind lidar, consisting of a coherent wind lidar from a Chinese manufacturer is presented in this manuscript. There are a few other papers on ship-borne wind lidars (e.g. Achtert et al. 2015 and from NOAA, e.g. Tucker et al. 2009) and thus this kind of application with its specific challenges (ship movement and environment) is challenging and still provides some novelty. In contrast to other earlier reports (e.g. Achtert et al. 2015), no active stabilisation of the complete lidar is performed, but the movement and angles are measured and corrected in post-processing. Some comparisons to radiosondes from a cruise in the Yellow Sea are shown in addition to two cases with vertical and horizontal wind measurements. Thus the topic of the manuscript fits to AMT. Major comments from my side are related to the description of the motion correction approach with GPS/INS, which is not clear at some places and lacks details to assess its novelty. Indeed the manuscript is very similar to the one of Achtert et al. (2015) in terms of description of methodology (correction algorithms), statistical comparison and evaluation with radiosonde, assessment of errors (spectral approach). Also numerous minor comments are related to the presentation of the topic. Thus I would recommend that the manuscript can be only accepted after major revisions of text, figures and additional material is included.

**General and Major Comments:**

**1.** The differences to the NOAA HRDL and the system by Achtert et al. 2015 should be mentioned more explicitly in the introductory paragraph (p. 3, 1st paragraph "it can be seen .." is not clear) Achtert et al. (2015) use an active motion-stabilized platform; so the difference to the described system here is clear. The NOAA HRDL uses a SDS to point the scanner LOS direction. But all systems need a motion-correction in the post-processing afterwards due to the limited accuracy of the active systems. So it is understood that the described system in the paper is neither on a motion-stabilized platform nor the scanner LOS pointing direction is controlled by use of the ship attitude angles. Is this correct? If yes, then also the limitations of this approach (e.g. high ship movements, rough sea) should be discussed in the main part and summary more explicitly. On the other hand it is mentioned on p. 9, ch. 3.2 that, "the hemispherical scanner maintains the pointing of the lidar beam to zenith stare mode..". Does that mean that the scanner direction is controlled by the information from the INS?

**R: The described system in the paper is neither on a motion-stabilized platform nor the scanner LOS pointing direction is controlled by use of the ship attitude angles. The LOS velocity measured by CDL in ship coordinate system $\vec{V}_{LOS\_measure}$ is unaffected by the ship movement, therefore the approach is available under high ship movement. $\vec{V}_{LOS\_measure}$. Since the bandwidth $B_{100}=(L-1)\Delta f=97.68$ MHz, the corresponding radial velocity measurement range is $\pm 37.5\ \mathrm{ms}^{-1}$. As for the feasibility under different sea condition, generally, except for the extremely rough sea condition, the LOS velocity component from vertical velocity in different directions is assumed to be identical. Then the $u$, $v$ can be calculated using a modified 4-DBS formula. Under extremely rough sea condition,**

the difference of elevation angle in different directions is significant, and the contribution of vertical velocity to LOS velocity needed to be treated carefully. In this case, the height interpolation of radial velocity can be used, and if three or more radial velocities at the same height are obtained, the horizontal and vertical velocity can be retrieved. But if the elevation angle in one direction is too small, the detectable height will be limited. Figure 1 shows the statistical distribution of the lidar pitch and roll angle from 09 May 2014 to 19 May 2014. In most cases the sea condition is less rough and the approach can be used reasonably.

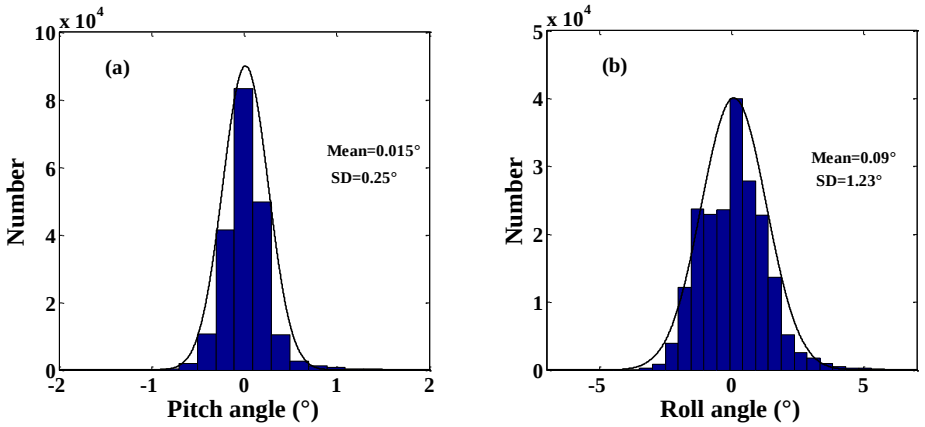


Figure 1. Statistical distribution of the lidar pitch and roll angle from 09 May 2014 to 19 May 2014.

I didn't explain it clearly, "the hemispherical scanner maintains the pointing of the lidar beam to zenith stare mode", in this sentence, the "zenith stare mode" represents the measurement in Lidar coordinate system, not the scanner direction in ECS controlled by the information from the INS?

2. The main part of the manuscript deals with the motion correction. Thus relevant parameters of the used GPS and INS system (type, accuracy, precision, data acquisition rate) should be provided and discussed. Why are 2 antennas shown in Fig. 1? Also the limitations of this approach, e.g. for high wind speeds or high angular rates during rough see conditions need to be discussed in the main text. Why did the authors not chose an approach the control the scanner LOS direction, especially for the vertical pointing mode, by using the attitude angles from the INS (or is this applied)? Also details of the hard-target calibration need to be discussed. Is this performed once (before the cruise)? What angular offsets are determined, are different hard-targets in different direction used (range, elevation)? It is stated that "It can be seen that there exists no laser direction error." How do you come to this conclusion? Can you provide more details on that (e.g. data, Figure)?

R: The CDL scanner is mounted on the roof of the cabinet container with two fixed Global Navigation Satellite System (GNSS) antennas. Double antennas are used for determining the exact heading angle with accuracy of $0.1^{\circ}$ when the ship is anchored. The attitude correction system uses XW-GI5651 MEMS Inertial/Satellite Integrated Navigation System. It is equipped with MEMS gyroscope, accelerometer, and multi-mode and multi-frequency GNSS receiver. It can realize single antenna dynamic alignment or

double antenna auxiliary fast and high-precision orientation. The specification are listed in Table 2. Generally, the attitude correction system uses GNSS to define earth coordinate system (ECS), where the ship speed, heading angle and earth location including the longitude and latitude in ECS can be obtained. Another important part of attitude correction system is the inertial navigation system. The inertial navigation system is rigidly mounted on the base of the scanner within the cabinet container, instead of the deck of the ship, to keep constant relative angles with reference to the lidar coordinate system. It records the lidar motion angles in real time including pitch, roll, laser beam azimuth and elevation even when the GNSS is sheltered or disturbed, and the recorded information is the exact lidar itself attitude in lidar coordinate system.

Table 2: Component Parameters of the XW-GI5651 MEMS Inertial/Satellite Integrated Navigation system.

| | | | | | | |
|---|---|---|---|---|---|---|
| System real-time precision | | | | | | |
| Heading | $0.1^{\circ}$ (double antenna mode, baseline length $\geq 2$ m) | | | | | |
| | $0.1^{\circ}$ (single antenna, speed > 10 $ms^{-1}$) | | | | | |
| Attitude | $0.1^{\circ}$ | | | | | |
| Position | Single point positioning $\leq 5$ m | | | | | |
| | RTK 2 cm + 1 ppm (CEP) | | | | | |
| Data updating rate | 200 Hz (configurable) | | | | | |
| Starting time | $\leq 10$ s | | | | | |
| Alignment time | 1~2 min (depending on dynamic maneuvering mode) | | | | | |
| | Double antenna aided orientation time $\leq 1$ min | | | | | |
| Post-processing precision | | | | | | |
| Heading | $0.05^{\circ}$ | | | | | |
| Attitude | $0.05^{\circ}$ | | | | | |
| Position precision | Time to lose lock | 0 s | 10 s | 60 s | 300 s | 600 s |
| | Position | 0.02 m | 0.04 m | 3 m | 20 m | 60 m |
| Physical properties | | | | | | |
| Power consumption | < 7 W | | | | | |
| Working temperature | -40 °C ~ 80 °C | | | | | |
| Overall size | 100 mm × 90 mm × 50 mm | | | | | |
| Weight | < 500 g | | | | | |

The limitation of this approach has been discussed in *General and Major Comments Question 1.* We didn't use any actively stabilized compensation device in order to simplify mechanical system and to easily place CDL on ship platform. What's more, the scanner control system needs higher accuracy, especially for vertical mode measurement.

In our system, the inertial navigation system is rigidly mounted on the base of the scanner, instead of the deck of the ship, to keep constant relative angles with reference to the transmitting laser beam. It records the Lidar motion angles including pitch, roll, laser beam azimuth and elevation, thus the recorded attitude information is the exact Lidar itself feature in Lidar coordinate system. After installation, a hard target calibration is firstly performed to determine the misalignment between the ship and laser beam axes. Specifically, the buildings near the wharf where there is no occlusion issue between the CDL and the candidate buildings can be chosen as the hard target. As shown in Fig.1, when the laser beam direction points to the hard target, the azimuth angle $\varphi_{lidar}$ in Lidar coordinate system is recorded, meanwhile the azimuth angle $\varphi_g$ in Earth Coordinate System can be obtained using the Google Earth software if the exact longitude and latitude of hard target is determined. According to the ship heading angle $\psi$, we can get the azimuth angle $\varphi_s = \varphi_g - \psi$ between ship heading and the hard target in Ship Coordinate System. So far, the misalignment angle between the ship and laser beam axes $\Delta\varphi = \varphi_s - \varphi_{Lidar}$ can be corrected using the geometrical relationship between these three angles. And then the standard ship attitude definition can be determined based on the relationship between Lidar and ship coordinate system, which will be used in the following ship motion correction process. It can be seen that there exists no laser direction error determined by misalignment between the ship and laser beam axes since the Lidar is considered to be relative static during field experiment.

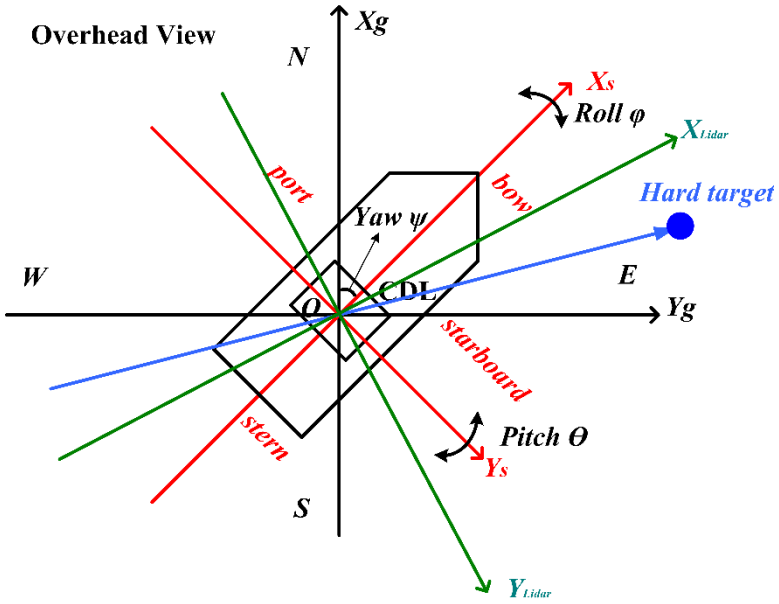


Figure 1. The overhead view of Lidar, ship and Earth coordinate system and corresponding hard target calibration.

3. The temporal resolution of the determination of the ship-induced Doppler shift (eq. 6) and the correction of the LOS velocity (eq. 7) needs to be stated and discussed. A figure

showing a time-series of raw-data from the sensors (angles, velocity) could illustrate this to provide an impression about the time scales of the ship movement during anchored and cruising measurements. Also the timing of the DBS is not clear: How long is 1 LOS obtained, how long for the vertical velocity, and how long is the averaging time for the horizontal wind? Especially for the vertical pointing measurements the variability of the off-zenith angle should be shown in a Fig. The vertical velocity determination does need a correction for the horizontal wind. What is the time separation between the horizontal and vertical wind measurement?

**Reply: Both the determination of the ship-induced Doppler shift and the radial velocity have the same temporal resolution of 0.5 s. Figure 4 in the revised version shows the flowchart of shipborne CDL data processing. Specifically, the LOS velocity and Signal to Noise Ratio (SNR) can be firstly determined using lidar data and FFT analysis. After the data pre-processing including the quality control based on SNR threshold, the attitude transformation is then used to obtain the azimuth and elevation in each LOS vector in Earth coordinate system with temporal resolution of 0.5 s. The LOS velocity detected by lidar is the atmosphere motion relative to ship coordinate system, thus the removal of the along-beam platform velocity due to ship motion is needed. In this study, the horizontal wind profile with 2-min temporal resolution will be retrieved for vertical velocity correction. Basically, the LOS velocities from $N$, $S$, $E$, and $W$ direction after SNR quality control during the chosen 2-min interval are collected firstly. Then the procedure of filtration of reliable estimates of each radial velocity based on SNR threshold is used to obtain "good" speed estimates. The selected radial velocities and corresponding ship condition information in each radial direction are averaged and the averaged ship condition will be used for the removal of platform velocity effect. Finally, the horizontal with 2-min temporal resolution can be retrieved using modified 4-DBS mode. The vertical wind measurement has a temporal resolution of 0.5 s, the horizontal wind whose retrieved time is closest to vertical wind measured time will be used for vertical velocity correction. A time-series of raw-data from the sensors (angles, velocity) and corrected angles can be seen in Fig.1 and Fig 2 as below:**

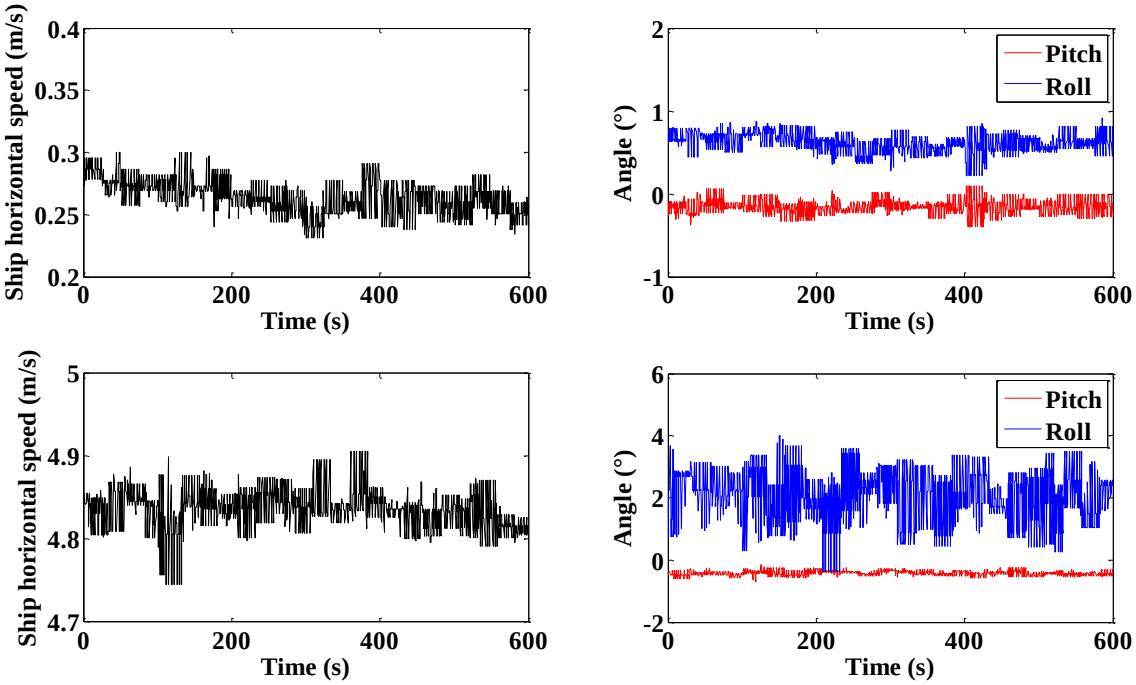


Figure 1: (a) Time series of ship horizontal speed and (b) pitch and roll angles on 09 May 2014 (15:52-16:02) during anchored measurement, (c) Time series of ship horizontal speed and (d) pitch and roll angles on 13 May 2014 (07:44-07:54) during cruising measurement.

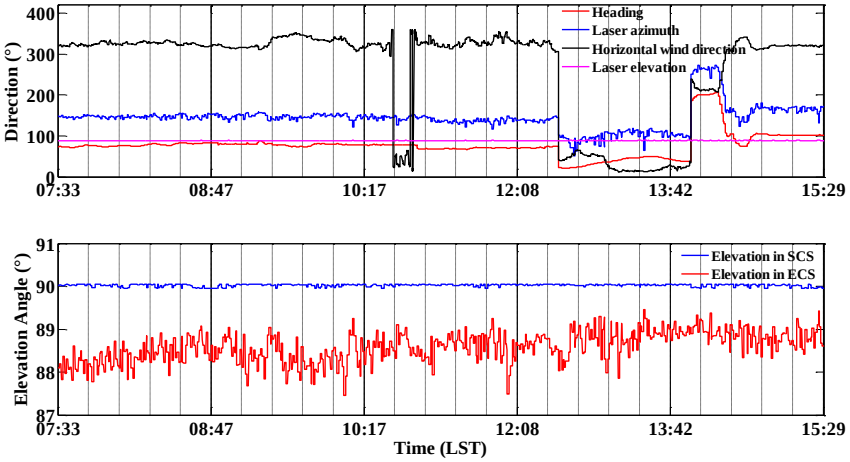


Figure 2: Example measurement from 07:33 to 15:29 LST 14 May 2014: (a) Time series of ship heading, CDL laser beam azimuth and elevation in the Earth coordinate system, and horizontal wind direction at 0.4 km. (b) Elevation angle in zenith stare mode in Ship Coordinate System and Earth Coordinate System.

4. In Achtert et al. (2015) the influence of the distortion of the flow due to the ship is discussed and modelled. In this manuscript this issue is only mentioned in 1-2 sentences on p. 9. What was the geometry/height of the ship? What would be the maximum height for a flow distortion, taking some numbers and scaling from the approach of Achtert et al (2015)? The lidar and radiosonde data is shown only above 150 m for this manuscript,

but you conclude from your statistical comparison that the height of 200 m might be still affected by the flow distortion. So some more discussions on the geometry/height of the ship and the expected flow distortion around is needed.

**R: The height of Dongfanghong-2 is 84 m. The relative height between CDL and the highest building on ship is about 15 m shown in Figure 1. When the strong wind blows from the ship bow, the building and experimental setups on ship have an important effect on CDL lower-level detection volume where the induced-turbulence may cannot meet the assumption of homogeneous isotropic atmosphere for 4-DBS retrieval. On the other hand, the blind area of CDL is 150 m and corresponds to the height of 129.9 m when laser beam elevation angle is $60^{\circ}$, meaning that less data points are available below 200 m with effective comparison. Therefore, whether the flow distortion around the ship is the main reason for the discrepancies in the lower part measurement or not is yet unclear. Further study, especially focused on the CFD model, needs to be used to the assess the potential effects on turbulent flow and wind field analysis.**
**In Achtert's paper, it is concluded that the normalized bias in horizontal wind speed is less than 2% for all wind directions at altitudes above 75m. But the specific geometric parameters of the ship in CFD simulation domain are not mentioned, which is important for determination of the maximum height for a flow distortion induced by ship. However, it surely provides us a new sight for Lidar data quality assessment, especially for the correction of the wind measurements used for turbulence fluxes exchange from Marine-Atmosphere interface.**

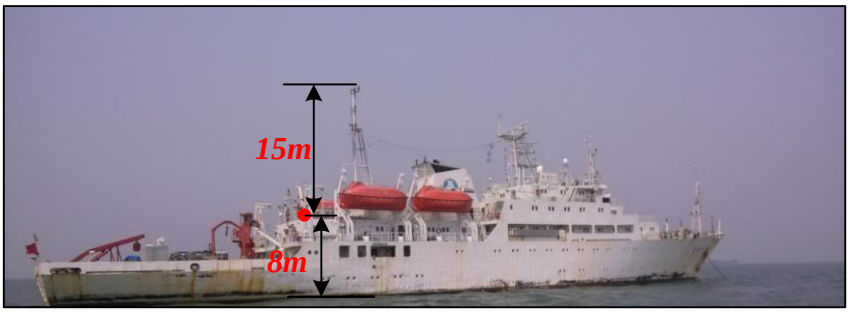


**Figure 1. The Dongfanghong-2 research vessel during 2014 Yellow Sea Campaign. The red solid dot represents the CDL position.**

5. Ch. 3.3. Error analysis: The authors deal here with the derivation of systematic errors (bias) to the horizontal wind retrieval I am wondering, if the error sources from the knowledge of the ship velocity and the lidar pointing angle are really systematic (over longer timescales) or random, and would add to the random error of the wind retrieval. A clear distinction needs to be made in the underlying assumption for the ship velocity and lidar pointing wrt systematic and random errors. Are the provided numbers for ship velocity and pointing only the systematic part? What would be the random error of these quantities?

**R: It is noted that the knowledge error of the ship velocity and lidar pointing angle mentioned in Part 3.3 are systematic part and it is assumed that the random error of these parameters is zero, which is reasonable and robust for horizontal wind retrieval.**

6) The authors could consider moving some of the equations related to the correction algorithms (Ch. 2) and error analysis (Ch. 3.3) to an appendix. At least for these parts, which are well known (e.g. coordinate transformations, descriptions of angles, DBS technique). I would restrict the description in ch. 2 and 3.3 to the novel aspects of this work.

**R: Thanks for your suggestion. The motion-correction algorithm including Eq. 1-5 in the manuscript has moved to Appendix A.**

7) I am missing a description of the overall objective of the deployment in the Yellow Sea in 2014 in the introduction. Was this only for technical demonstration, or were further atmospheric-oceanic processes studied. I am also missing a discussion of the open questions for turbulent flux measurements or wind vector measurements over the sea, which would need a shipborne Doppler wind lidar. One should discuss some objectives for the development of a shipborne wind lidar in the introduction. Also it might be useful to provide a paragraph in the Summary about future plans and campaigns.

**R: Thanks for your suggestion. The description of the objectives has been added to the last paragraph in the Introduction part. It is described below:**

**"The experimental investigation was undertaken by Dongfanghong-2 research vessel affiliated with Ocean University of China in 2014 over the Yellow Sea. The Yellow Sea, a marginal sea of the Pacific Ocean, is the northern part of the East China Sea. It is located between mainland China and the Korean Peninsula. There is seldom study on boundary layer dynamics study based on CDL in this region. As one of the main objectives, the CDL was deployed on the ship in this campaign to demonstrate the feasibility of the algorithm-based attitude correction method. The obtained accurate three-dimensional wind information can provide significant preparation for further studies on characteristics of dynamics and thermodynamics in the MABL and turbulence flux exchange over sea surface. In addition to CDL, as another important part of this campaign, a High Spectral Resolution Lidar (HSRL) and a CL31 ceilometer were also deployed on the ship platform in order to detect MABL height spatial-temporal evolution and to retrieve the aerosol and cloud optical characteristics such as extinction coefficient and backscatter ratio and so forth. It will help us to understand the complex behavior of MABL and the aerosol cloud forcing characteristics over sea region and the impact on climate change. This paper focuses on CDL performance and gives a thorough analysis of the attitude correction for lidar velocity measurement."**

**The description of the further plan has been added to the last paragraph in the Summary part. It is described below:**

**"Overall, combining a CDL with attitude correction system and accurate motion correction process as presented here forms a reliable and autonomous set-up that could be placed on mobile platform to provide more detailed, higher spatial and temporal resolution view of three-dimensional wind field information. It will be**

further validated and improved under different sea conditions using CFD model simulation and field campaign. More specific studies are being carried out or prepared, including atmospheric turbulence characteristics statistics and multi-scale wind field observation in MABL, wind turbine wake and atmospheric turbulence interaction over offshore wind power field (Wu et al., 2016; Zhai et al., 2017), mass transport and flux analysis in MABL with combination of CDL and Multi-wavelength Polarization Raman Lidar (Wu et al., 2016).

**Specific Comments**

1). p.1 Intro: A number of studies are referenced for turbulent fluxes over the sea surface (Axford, 1968). Could these studies be grouped by objective, technology or geographical region to be more specific. Otherwise this long list of references is not very informative.

R: Thanks for your suggestion. The references has been grounded according to different platforms and geographical region. It is shown below:

"There are many studies on the turbulent fluxes measurement over the sea surface. Various motion sensing technique on the moving platform has been developed in the field of airborne (Axford, 1968), space-borne (Hawley et al., 1993) and shipborne observations (Fujitani, 1992; Song et al., 1996; Edson et al., 1998; Miller et al., 2008). Many shipborne field experiments have been widely carried out over Pacific Oceanic area (Mitsuta et al., 1974; Bradley et al., 1991; Shao, 1995; Tsukamoto et al., 1995)."

2). p.3, line 15: "Few studies .. in this region". Are there any references for these studies?

R: As far as we know, there is seldom study on boundary layer dynamics study based on CDL in this region.

3). p. 5, L 11: The different elevation angles are probably due to ship rotation and movement during the time period of measuring different LOS directions, which should be stated here. Thus it is important to mention the duration of the measurement of each LOS direction, and the complete 4 beams, and the relevant movements of the ship during these periods. How is the expected elevation angle _0 obtained?

R: Thanks for your suggestion, The description has been added in the manuscript. It is shown below:

But for the shipborne platform, the elevation $\theta_g$ in four directions (north, south, west and east in ship coordination system) may have slightly difference (see Eq. (A5)) due to ship rotation and movement during the time period of measuring different LOS directions, thus a conversion of $\vec{V}_{LOS}$ from real elevation $\theta_g$ to the expected elevation $\theta_0$ is firstly processed, that is,

$$\vec{V}'_{LOS} = \vec{V}_{LOS} \cos\theta_0 / \cos\theta_g \quad (4)$$

It is noted that $\theta_0$ can be set any value from $0^\circ$ to $90^\circ$, and in this paper $\theta_0 = 60^\circ$ is set for horizontal wind profile retrieval. During the experiment, each radial direction will take 5 s to obtain 10 measured LOS velocity for accumulation and

average. In this sense, the highest temporal resolution of horizontal wind velocity using 4-DBS mode is 20 s. The recorded ship condition information has the same update rate of 0.5 s as radial velocity's, which can be averaged to remove the platform motion effect on radial velocity.

4). p. 7, 1st paragraph: It should be stated, how the background noise signal is obtained, e.g. via the recorded signal after a sufficiently long laser travel time, or via a separate measurement w/o laser pulse emission. Do the authors see an advantage of their SNR definition over the one from Banakh et al. 2013?

R: The SNR in this study is defined as the ratio of the peak value of FFT spectral signal in each range bin to the Root-Mean-Square (RMS) of background noise signal. Figure 1 shows the array of the spectral $S(l\Delta f;k\Delta R)$, where $l=0,1,2,3,...,L-1$ is the spectral channel number and $L=100$. In this case the frequency resolution $\Delta f \approx 0.98$ MHz and the corresponding velocity resolution is $\Delta V = 0.76$ ms$^{-1}$. The bandwidth $B_{100}=(L-1)\Delta f = 97.68$ MHz, and the corresponding radial velocity measurement range is $\pm 37.5$ ms$^{-1}$. Figure 1a shows the last 10 range gates raw array of spectral in green line. We estimate the averaged background noise spectrum

$$\overline{S}_N(l\Delta f)=\frac{1}{10}\sum_{k=94}^{103}S(l\Delta f;k\Delta R) \tag{8}$$

Substracting the background noise spectral $\overline{S}_N(l\Delta f)$ from the raw spectral array $S(l\Delta f;k\Delta R)$, the unnoisy array of spectral $S(l\Delta f;k\Delta R)$ can be obtained and shown in red line in Fig. 1. The peak value index $l_{peak}$ from the $S(l\Delta f;k\Delta R)$ can be firstly obtained and thus the absolute signal power $P_s(k\Delta R)$ at various ranges $k\Delta R$ can be represented as:

$$P_s(k\Delta R)=S(l_{peak}\Delta f;k\Delta R)-\frac{1}{12}\left(\sum_{l_{peak}-20}^{l_{peak}-15}S(l\Delta f;k\Delta R)+\sum_{l_{peak}+15}^{l_{peak}+20}S(l\Delta f;k\Delta R)\right) \tag{9}$$

Replacing integration by summation and taking into account that the zero velocity point in one channel is $l_{zero}=50$, we estimate the noise power $P_N$ as

$$P_N=\frac{1}{10}\sum_{k=94}^{k=103}\sqrt{\frac{1}{21}\sum_{l=l_{zero}-10}^{l_{zero}+10}\hat{S}_N(l\Delta f;k\Delta R)^2} \tag{10}$$

Finally, we obtain the range profile of the $SNR(k\Delta R)$ using the equation

$$SNR(k\Delta R)=10\log_{10}\left(\frac{P_s(k\Delta R)}{P_N}\right) \tag{11}$$

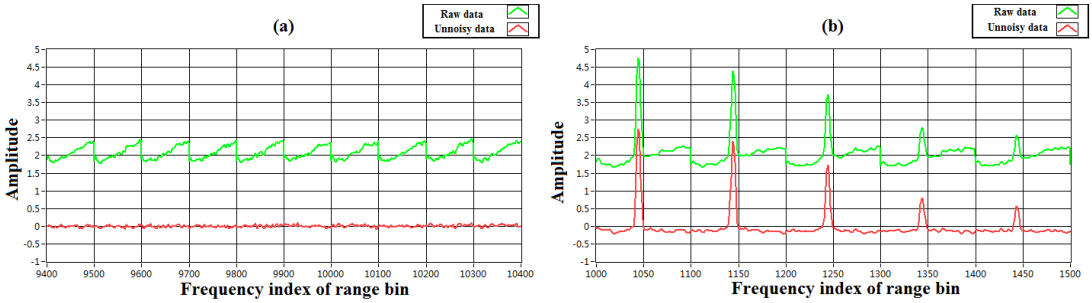


Figure 1: The CDL measured array of the FFT spectra (a) the last 10 range gates spectra for background noise spectrum estimation (b) the 1st – 5th range gates (150 m – 270 m, range resolution

is 30 m) spectrum.

The SNR from Banakh et al. 2013 is defined as the ratio of the averaged heterodyne signal power $P_s$ to the average detector noise power $P_n$ in a 50-MHz bandwidth. The power $P_s$ and $P_n$ are integrals of the spectral densities $S_s(f)$ and $S_n(f)$, respectively, in frequency f within a band of width $B_{50}$, that is:

$$P_s = \int_{B_{50}} S_s(f)df \quad (5)$$

$$P_n = \int_{B_{50}} S_n(f)df \quad (6)$$

Comparing the definition from Banakh et al. 2013, the SNR in this paper is simpler and also indicates the CDL detection capability, data accuracy and atmospheric tracer particle relative intensity. In this sense, the SNR threshold value in this paper is higher than the one in previous studies (Banakh et al. 2013; Achtert et al 2015) for the same signal power spectrum.

5). p. 7, L24: It should be described how the wind fluctuations are determined. Is it the standard deviation of wind measurements of higher temporal resolution (resolution?) during the 10 min.? Why are bars shown only for part of the profile in Fi.g 4 and 5? Is it smaller than a specific value below 1.4 km in Fig. 4? Do the fluctuations represent instrument noise or atmospheric fluctuations? What could be the reason that there are higher fluctuations in the layer of 1.4-1.6 km in Fig. 4?

R: The black line indicates the mean measurement by CDL during the 10-min period, and the red line shows the result which is obtained from simultaneous radiosonde data. The blue bars represent the standard deviation of CDL wind measurement from the 2-min temporal resolution results during the chosen analyzed period, representing the atmospheric fluctuations.

The standard deviation of wind speed and direction below 1.4 km are less than 0.5 m/s and 5°, respectively, showing that the atmospheric condition is relative stable below 1.4 km. While there are higher fluctuations in the height of 1.4 – 1.6 km. The higher SNR in the layer of 1.4 – 1.6 km shown in Fig. 5a implies the existence of cloud or aerosol layer, more active and complex atmospheric movement in this layer may results in higher fluctuations.

6). p. 7, L27: Same question related to the method to determine the STD for the angles. Determined from the variability during the 10 min using raw data with of temporal resolution of xx s?

R: I didn't explain it clearly. The related description has added to the manuscript, and it is shown below:

It is noted that the standard deviation of the angles is determined from the variability during the 10 min period using N=1200 raw data with temporal resolution of 0.5 s, which is shown in Fig. 7b.

7). p.7, L28: Which SNR threshold was used here?

**R: The SNR threshold in this study is 8 dB. The reason why SNR threshold is 8 dB has been analyzed in Sect. 3.3.**

8). p.8, L26, last sentence: What is a "multipath effect"? This should be clarified. Also the difference in radiosonde and lidar location should be stated quantitatively. What is the difference in mean wind speed and direction between radiosonde and lidar above 1 km? Can a lidar instrumental effect excluded to explain the difference? I am not convinced that it is only colocation.

**R: The difference in mean wind speed and direction between radiosonde and CDL above 1 km is about 3.4 $ms^{-1}$ and 15.2°, respectively, showing significant discrepancy. On the one hand, the random error of the corrected CDL estimation of the wind due to the low SNR shown in Fig. 6a contributes to this discrepancy. On the other hand, according to the recorded information, the mean heading angle and cruising speed of the ship is 75.86° and 4.84 $ms^{-1}$, respectively, and the mean wind speed and direction above 1 km is 255° and 18.4 $ms^{-1}$, respectively. Since the drift of radiosonde is affected by atmospheric wind, and turbulence perturbation and the CDL detection volume is changing during cruising observation, the result discrepancy between radiosonde and CDL caused by different observation location, also called the multipath effect, is larger with increasing height.**

9). p.8 and Fig. 6: I would propose to plot the radiosonde on the x-axis and the lidar on the y-axis and also perform the linear least square fit with these coordinates. I consider the radiosonde as more accurate and the usual linear LSF procedures assume that the x-parameter is without errors (minimization of vertical differences). I also consider the criteria of excluding data with 1*SD as too strict. Only gross outliers – deviating from a Gaussian distribution – could be excluded. This would typically result in a criteria of >3*SD. It needs also to be stated, how many data-pairs were excluded from the statistical comparison in order to judge the numbers of gross outliers. Also the SD typically refers to the SD of the difference (lidar-radiosonde). I am wondering how the SD of the lidar data ydata was obtained here. It is clear that the statistical parameters for bias, SD, R, and RMSE need to be calculated without a rigorous excluding of the data (with 1*SD). This point needs to be revisited and clarified.

**R: I agree with your suggestion, the radiosonde on the x-axis and the lidar on the y-axis has been used in the manuscript. Figure 1 shows the distribution of difference (lidar-radiosonde) and fitted Gaussian distribution. The total number of wind speed and direction dataset is 1062 and 951, respectively. The 1*SD, 2*SD, 3*SD are plotted in red, black and blue dotted-line, respectively. The SD is the standard deviation of the difference of (lidar-radiosonde). It can be seen from figure 1 that the criteria of excluding data with 2*SD is more reasonable for gross outliers. Figure 2-4 shows the comparison of lidar and radiosonde using different criteria. The excluded data-pair using the different criteria are listed in Table 1 below:**

**Table 1. Excluded data-pair and corresponding % using different criteria**

| | Excluded wind speed data-pair (%) | Excluded wind direction data-pair (%) |
|---|---|---|
| 3*SD | 14 (1.3%) | 12 (1.3%) |
| 2*SD | 62 (6%) | 56 (5.9%) |
| 1*SD | 252 (21%) | 225 (24%) |

The statistical parameters for bias, SD, R, and RMSE after data quality control with different criteria are shown in figure 2-figure 4.

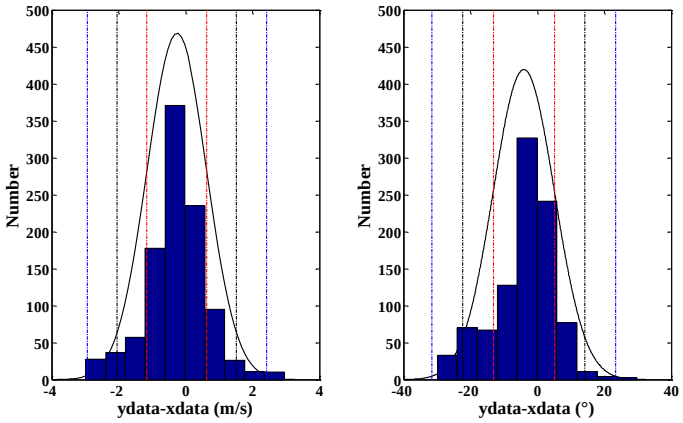


Figure 1: Distribution of difference (lidar-radiosonde) (a) wind speed (m/s) (b) wind direction (°)

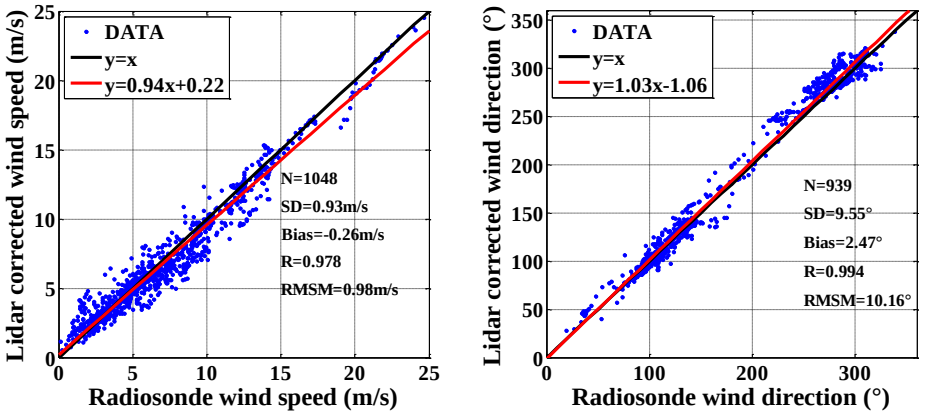


Figure 2: Comparison of (a) wind speed and (b) wind direction between CDL and radiosonde data using 3*SD threshold

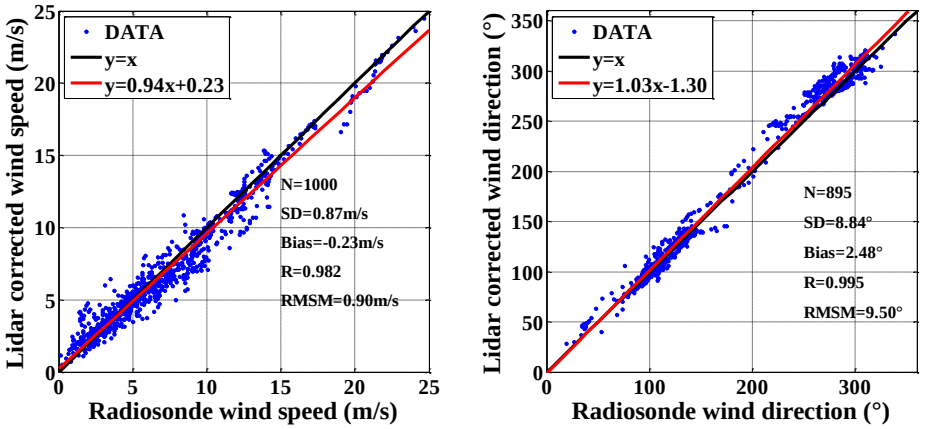


Figure 3: Comparison of (a) wind speed and (b) wind direction between CDL and radiosonde data

using 2*SD threshold

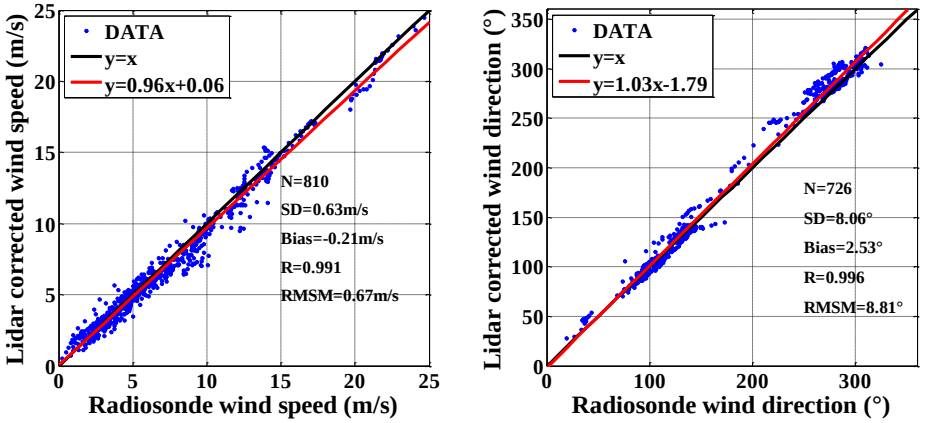


Figure 4: Comparison of (a) wind speed and (b) wind direction between CDL and radiosonde data using 1*SD threshold.

10). p.9, ch. 3.2 and Fig. 7: The dots for MABL height are shown for the first 1/3 of Fig. 7 in a region of SNR around 10, where no obvious gradients can be seen, whereas for the second 2/3 it is more in the region between 10 dB (light blue) and 0 dB (dark blue). Please check and comment. Is there a reference about the ABL height determination using the first negative gradient?

R： We didn't explain it clearly. The MABL height has been retrieved and compared using different instruments such as the CDL, radiosonde, and CL31 ceilometer during this campaign (Wang et al., 2016). Many papers have discussed the use of backscatter signal of Lidar for boundary layer height estimation, assuming that the boundary layer has higher aerosol concentrations than the free troposphere above. In this paper, the SNR, representing the relative aerosol backscatter profiles, were used and two common methods includes thresholding SNR to determine MABL height (Melfi et al. 1985) and finding the height of the first strong negative gradient (White et al. 1999; Hennemuth and Lammert 2005 ) in SNR. Figure 1a shows the Time-Height-Intensity of SNR and the retrieved MABL height marked with black and red solid circles. The radiosonde data during 17:34 LST 14 May 2014 and corresponding MABL height using the gradient of potential temperature and relative humidity are also shown in Fig. 2. It can be seen that diurnal variation of MABL height is less obvious within 1.0 km - 1.5 km, consistent with the mixing layer height retrieved from the radiosonde potential temperature and relative humidity profile.

The related references have been added to the manuscript:

1. Hennemuth, B., and Lammert, A.: Determination of the atmospheric boundary layer height from radiosonde and lidar backscatter, Boundary-Layer Meteorol., 120(1), 181-200, 2006.

2. Menut, L., Flamant, C., Pelon, J., and Flamant, P. H.: Urban boundary-layer height determination from lidar measurements over the Paris area, Appl. Opt., 38(6), 945-954, 1999.

3. Wang, D., Song, X., Feng, C., Wang, X., and Wu, S.: Coherent Doppler Lidar Observations of Marine Atmospheric Boundary Layer Height in the Bohai and Yellow Sea, Acta Opt. Sin., 35(A01), 1-7, 2015.

4. White, A. B., Senff, C. J., and Banta, R. M.: A comparison of mixing depths observed by ground-based wind profilers and an airborne lidar, J. Atmos. Oceanic. Technol., 16(5), 584-590, 1999.

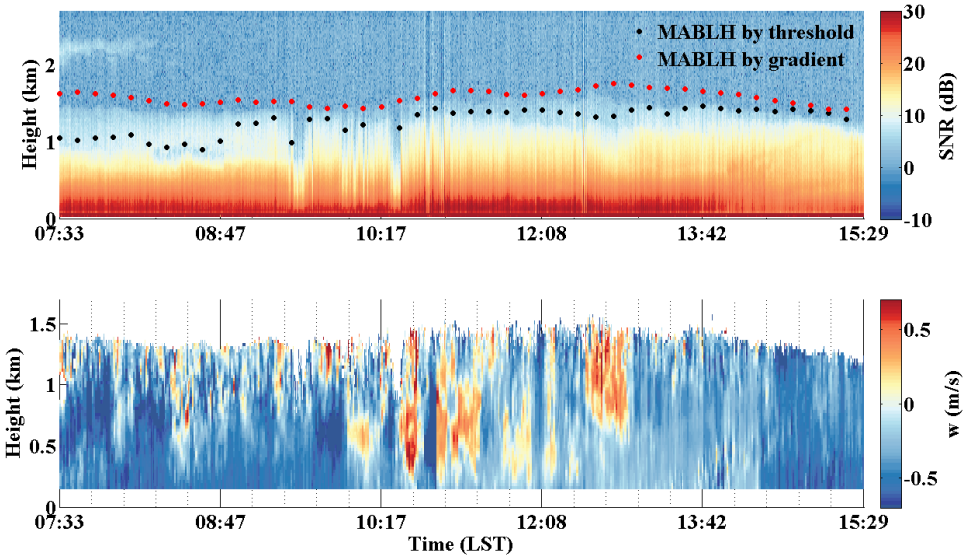


Figure 1: Example measurement from 07:33 to 15:29 LST 14 May 2014: (a) Time-Height-Intensity of SNR and retrieved MABL height using SNR threshold and gradient method (black and red solid circles, respectively). (b) Time-Height-Intensity of vertical velocity after attitude correction.

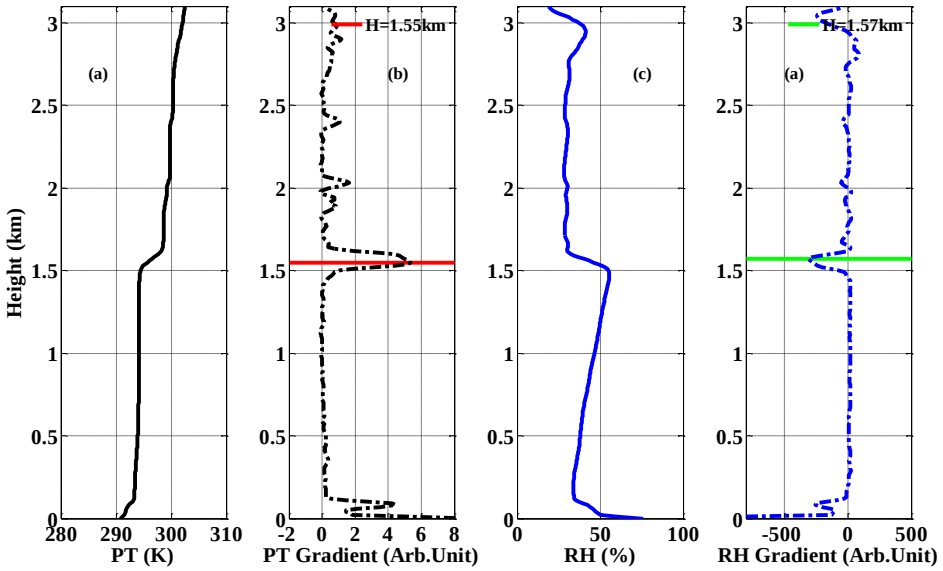


Figure 2: Radiosonde profiles of (a) potential temperature (K) (b) the gradient of potential temperature (c) relative humidity (%) and (d) the gradient of relative humidity at 12:00, LST 14 May 2014. The horizontal red and green lines in (b) and (c) stand for MABL height retrieved from potential temperature and relative humidity, respectively.

11). p.11, L5: I consider an error of only 0.1_ for the ship heading as very small. Is this justified by the hard-target measurements?

**R: The error of 0.1 for ship heading comes from the accuracy of Global Navigation Satellite System.**

12). p.11, L8: What quantity is derived in eq. (14) in comparison to eq (13); Both are called "bias" LOS_N but eq. (14) with a "N'". Text should clearly state, the difference. What eq. (13 or 14) is then used in the estimates for the bias (eq. 17 and 18)?

**R: The $\vec{V}_{LOS}$ is the LOS velocity in Earth coordination system with elevation $\theta_g$. The $\vec{V}'_{LOS}$ is the LOS velocity in Earth coordination system with elevation $\theta_0 = 60^\circ$ in this study. The relationship between $\vec{V}_{LOS}$ and $\vec{V}'_{LOS}$ is $\vec{V}'_{LOS} = \vec{V}_{LOS}\cos\theta_0 / \cos\theta_g$. The bias of $\vec{V}_{LOS}$ is derived using eq (13) and the bias of $\vec{V}'_{LOS}$ is affected by $\vec{V}_{LOS}$ and $\theta_g$ according to the error propagation theory, as shown in eq. (14). The estimation for horizontal wind bias shown in eq. 17 and 18 are related to $bias_{b1}$ and $bias_{b2}$. According to $b_1 = (\vec{V}'_{LOS\_N} - \vec{V}'_{LOS\_S})/\cos\theta_0$ and $b_2 = (\vec{V}'_{LOS\_E} - \vec{V}'_{LOS\_W})/\cos\theta_0$, the bias of $\vec{V}'_{LOS}$ will be used.**

13). p.11, eq. 15/16: These eq. could be moved to ch. 2 after eq (10), because it deals with u, and v retrieval and not with error estimates as in ch. 3.3.

**R: Thanks for your suggestion, the eq 15-16 has moved to ch.2 after eq.10.**

14). p.11, L13: Here it is stated, that the lidar pointing angles are very small (and assumed to be perfect), but on p.12, L2 it is stated the errors are dominated by ship velocity and lidar pointing errors. This is in contradiction.

**R: I did not explain it clearly. Because of the requirement for small bias in the radial velocity measurements, the error in the laser beam direction must be very small and one can assume perfect knowledge of the coefficient $a_i$.**

**The dominant source of bias of the horizontal velocity estimates come from the biases of the radial velocity estimates, which are determined by the error in the ship velocity $\vec{V}_{ship\_horizontal}$, $\vec{V}_{ship\_vertical}$ and heading angle $\psi$ and lidar pointing knowledge errors $\Delta\varphi$ and $\Delta\theta$ (see Eq. 13).**

15). p.12, L6ff: Here the method of obtaining the random error is described ("In this case, a"). But no resulting spectrum is shown in Fig. 9. This needs to be added or reformulated.

**R: Various methods of estimating the magnitude of the random error of Doppler Lidar velocity measurements have been introduced (Frehlich 2001). The measurement of error from velocity spectrum were used in this paper. A 50 % window overlap factor, a Hamming window is used in order to reduce the leakage in the spectra. A zero-padding of the missing values were applied to each window for each spectrum calculation to improve the frequency resolution. The constant high-frequency region of velocity spectrum higher than 0.2 Hz, shown in figure below, represents uncorrelated random**

error contribution, which is departing from the Kolmogorov's -5/3 law. The random error of vertical wind velocity is estimated as the standard deviation of the measured signal after high-pass filter.

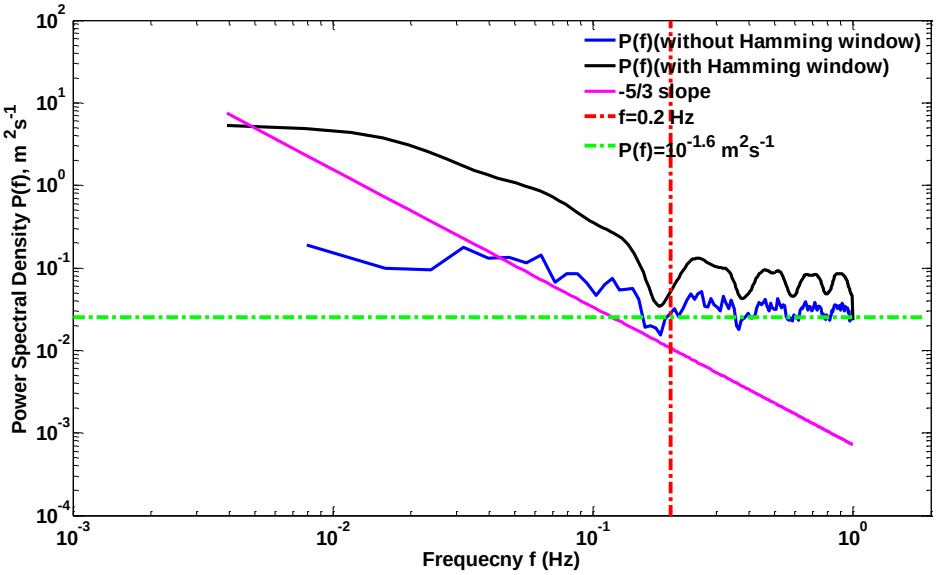


Figure 1: Power spectral density P(f) without and with Hamming window for the CDL measured vertical speed between 15:52 and 16:02 LST on 09 May and for an altitude of 1495 m (blue and black solid line, respectively). The expected spectral behaviour according to the Kolmogorov's−5/3 law (pink solid line), the noise frequency threshold (red dotted line) and the derived noise floor for the CDL ( green dotted line) are shown.

16). P12: L12: Are you sure that it is an elevated aerosol layer and not a cloud, which provides the high SNR around 1.5 km?

R: Thanks for your suggestion. Actually, we cannot judge whether it is an elevated aerosol layer or cloud only using the SNR intensity signal. We searched the recorded information from Vaisala CL31 ceilometer software screenshot, as shown below:

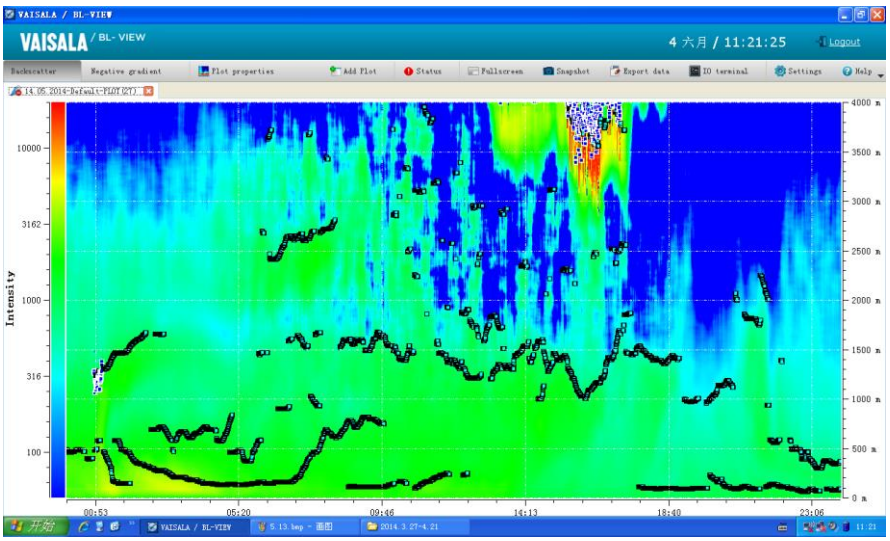


Figure 1: CL31 ceilometer software real-time results on 14 May 2014.

**In this figure, the candidate boundary layer height and cloud base height can be marked with black squares and white squares, respectively. The high SNR around 1.5 km during 07:33 – 08:40 LST is an aerosol layer, not cloud layer. The description has been corrected in the manuscript.**

17) p.12, L23: speckle-induced phase noise is not discussed in Achtert et al. 2015. Another reference needs to be provided

**R: The related references have been added to the manuscript.**

**1. Frehlich, R.: Effects of wind turbulence on coherent Doppler lidar performance, J. Atmos. Oceanic. Technol., 14(1), 54-75, 1997.**

**2. Frehlich, R.: Estimation of velocity error for Doppler lidar measurements, J. Atmos. Oceanic. Technol., 18(10), 1628-1639, 2001.**

18). p.13 Summary: The limitations of the approach in comparison to existing systems need to be mentioned in the summary. Also I am missing an outlook about future algorithm or hardware improvements or future deployment during ship cruises.

**R: The limitation of the approach has been discussed in** General and Major Comments Question 1.

**The outlook has been described in** General and Major Comments Question 7.

19). p.13, L14: The number for the bias and the STD from the statistical comparison of all radiosondes should be stated here.

**R: The total number of wind speed and direction dataset for comparison is 1062 and 951, respectively.**

20).Ref. Liu et al. 2010: More details should be provided for this reference, which is not really accessible, or the reference should be removed or replaced. Also Achtert et al. (2015) provide these transformations.

**R: In Liu et. al 2010 paper, a mobile Doppler lidar had been developed for 3D wind measurements by Ocean University of China. In order to further improve the mobility of the mobile Doppler lidar for lidar calibration and validation, both GPS and inertial navigation system were integrated on the vehicle for performing measurements during movement. The modifications of the system and the results of the moving measurements were presented. This work simplifies the construction of the mobile Doppler system and makes the lidar more flexible for ground-based wind measurements and validation with the ADM-Aeolus spaceborne Doppler lidar.**

21).Fig. 1: An additional Figure should be shown of the ship to illustrate the location of the CDL on the ship and possible disturbances of the flow.

**R: Revised**

22).Fig. 1: The location of the INS on the CDL should be indicated in the Figure.
**R: Revised**

23).Fig. 2: The symbols used for the angles pitch, roll, yaw should be placed also in the Figures.
**R: Revised**

24).Fig. 7: the legend within Fig. 7b is too small
**R: Revised**
**%%==========%%**
Editorial: A large number of editorial comments were directly added to the PDF-Version of the manuscript. In addition the term “et al” needs to be replaced by “et al.”. The manuscript needs thorough proof-reading after revision.

1). P2 L27: “High Resolution Doppler Lidar (HSRL)” needs to be corrected also at other places
**R: Revised**

2).P4 L25: Check style file or other papers, if "," or ";" is needed to separate coordinates.
**R: Revised,** $X_g, Y_g, Z_g$

3).P5 L3: This is not clear: why is the azimuth angle changing, when looking downward.
**R: From the top view, the $\varphi_s$ increases in a clockwise direction during 4-DBS mode operation.**

4).P5 L4: This must be the Xs-Zs plane.
**R: we have checked the definition, it is the Xs-Ys plane.**

5).P5 L8: Here the indices "g" are missing.
**R: the “g” has added to the manuscript**

6).P6 L10: "homogenous" flow instead "cellular"
**R: revised**

7).P6 L17: N, S, E and W, not uppercase style.
**R: revised**

8).P8 L15: sentence not completed: “What’s more, the fluctuation in wind speed and direction above 1 km is more severe.”
**R: What’s more, the fluctuation in wind speed and direction above 1 km is more severe than the results below 1 km.**

9).P9 L3: “the coefficient of determination of 0.96”, I assume this value is R^2. I consider it sufficient to provide R.

**R: Yes, the coefficient of determination of 0.96 is R^2, the description is delated in the manuscript.**

10).P20 Fig 7. This text is too small; also the quantities should be plotted with differetn y-scales to see more details.
**R: revised, please see figure 11 in the revised vision.**

11).P23 Table 1 could be replaced by power consumption.
**R: revised**

12).P24 Table 2 are these numbers accuracy and precision?
**R: Yes, revised.**

13).P24 Table 3: I would consider only 2 significant digits for normalized RMSE and direction values as sufficient, e.g. 4.6 (instead 4.55) or 4.3 (instead 4.27)
**R: revised.**

14).In addition the term “et al” needs to be replaced by “et al.”. The manuscript needs thorough proof-reading after revision.
**R: revised.**